GI_Forum 2020, Issue 1
Page: 73 - 88
Full Paper
Corresponding Author:
t.schneider@fh-kaernten.at
DOI: 10.1553/giscience2020_01_s73

Towards Predicting Vine Yield: Conceptualization of 3D Grape Models and Derivation of Reliable Physical and Morphological Parameters

Thomas Schneider[1], Gernot Paulus[1] and Karl-Heinrich Anders[1]
[1]Carinthia University of Applied Sciences (FH Kärnten), Austria

Abstract

In viticulture, yield prediction plays an important role, helping winegrowers to predict the start of the next growth stage of vines and to improve vineyard management decision-making. To predict a vineyard's yield, it is necessary to gather accurate local information about the vine's phenology and morphology, such as the volume of individual grapes. Traditional collection of these data and yield prediction rely on resource- and time-intensive direct visual and manual in-field work by viticulturists. Thus, only limited sampling in the vineyards is possible, carried out by humans. Automated procedures utilizing sensor-based systems reduce the data acquisition time and enable the collection of high-resolution data from the entire vineyard. Large-scale 3D models of vineyards can be generated from these data and used to analyse, for example, the vineyard's yield or the vegetative stage of individual vines.

We propose a concept for a 3D model that uses close-range photogrammetry. In a laboratory experiment, we tested the acquisition of multi-view image datasets from grapes using close-range photogrammetry and derived physical and morphological parameters from 3D grape models. The results could contribute to the design and implementation of a large-scale in-field experiment.

Keywords:

precision viticulture, vine, 3D grape model, physical parameters, morphological parameters

1 Introduction

Vines play an important role in the lives of many, and their connection to mankind can be traced back to ancient times (Poupin et al., 2011). About 28.4 million litres of wine were produced in 2015, an increase of 3.5% since 2014 (Wine Institute, 2019). Due to the constantly increasing consumption and demand for high-quality wines, winegrowers need to find efficient approaches to guarantee effective vine-growing and high-quality grapes. To facilitate efficient and high-quality viticulture, vineyard managers record phenological data of their vines on a weekly basis (Westover, 2018). The knowledge gained through analysis of phenological data

helps them to execute vineyard management practices at the right time and to determine the beginning of the next growth phase of the plants (Westover, 2018). Furthermore, estimated crop yields derived from phenological information is also helpful for wineries so that they can predict better the size of their crops and how much wine they will produce (Moyer and Komm, 2015). However, phenological data collection is traditionally performed manually (Moyer and Komm, 2015), is time-consuming (Nuske et al., 2014), and can be prone to human error (Rose et al., 2016). The application of sensor-based systems to collect and analyse phenological data can help to avoid gaps in phenological datasets (Westover, 2018), reduce human error and data collection time, make yield prediction more reliable, and reduce labour costs (Rose et al., 2016).

This preliminary study deals with the conceptualization of 3D models of harvest-ripe grapes using close-range photogrammetry and the derivation of physical and morphological parameters from the models. It was conducted in the form of a laboratory experiment.

The knowledge from this study could be utilized for the design and implementation of in-field experiments at vineyard scale. Furthermore, the information obtained helps to evaluate how well empirical physical and morphological measurements of the phenological stages of vines (in this case from harvest-ripe grapes) compare to model-based measurements. Our study also provides data on the image resolution required to create 3D high-density point clouds of individual grapes from images taken by unmanned aircraft system (UAS) flight missions.

2 Precision Viticulture, Phenological Stages of Vines and Yield Prediction

2.1 Precision Viticulture

Scientists and viticulturists strive constantly to find new approaches to improve the efficiency of vineyard management and to increase the quality of grapevines. Rapid advances in the 20th and 21st centuries have provided new digital and spatial technologies and enabled new sciences with a focus on viticulture, including precision viticulture. Nowadays, sensor-based systems are often used in viticulture, for example to derive phenological data from vineyards (Rose et al., 2016) or to predict a vineyard's yield (Nuske et al., 2014).

Precision viticulture is defined as the application of geospatial technologies, devices and tools which exploit spatial location to collect, store, manipulate, analyse and visualize environmental data from vineyards. Technologies and systems developed through precision viticulture give winegrowers and viticulturists the opportunity to collect data from their vineyards in real-time with accurate positional information (Goldammer, 2015).

Thus, the application of precision viticulture technologies has a wide range of advantages for viticulture experts. The foremost advantage is the improvement of viticulture management, including not only the enhancement of management techniques but also the ability to improve decisions on when to apply particular techniques. Deploying vineyard-related practices in timely fashion, such as the adjustment of canopy and nutrients, or the detection and elimination of diseases and insects, leads to an increased yield, yield quality and yield security.

Furthermore, it helps to reduce operating costs and the use of chemicals, and to improve the quality of soil and groundwater around a vine (Maniak, 2004).

2.2 Phenological Stages of Vines

In the context of viticulture management and yield prediction, the topic of "phenology" plays an important role. Phenology is the science which focuses on the natural changes and development of organisms and their relationship with seasonal variations in climatic parameters (Centinari, 2018; Westover, 2018; Hellman, 2003). It gives winegrowers crucial information about the health and condition of their plants. An important phenological characteristic of vines are their vegetative changes and developments over the course of a season. The weekly collection of phenological data such as plant growth information is recommended in order to avoid gaps in the datasets (Westover, 2018). One difficulty in trying to measure a vine's phenology is that plant growth is an ongoing process, and individual vines have their own natural growth patterns which are influenced by many different factors. Thus it is difficult to divide the seasonal growth of vines into exact, discrete, phases.

Various scales and classification systems support winegrowers and scientists by dividing the growth process into several phenological stages. A frequently used phenological classification for vines is the Modified Eichhorn-Lorenz (E-L) system. This system was originally designed by Dr. K. W. Eichhorn and Dr. D. H. Lorenz in 1977, revised in 1995 by B. G. Coombe, and modified further in 2004 by Coombe and P. Dry, becoming known as the Modified Eichhorn-Lorenz system (Westover, 2018). The modifications of the original E-L system concern changes in the classification of bud growth, since the visual characteristics in the early stages of bud growth vary among grapevine varieties (Centinari, 2018).

The Modified E-L system classifies the annual growth of vines into 47 vegetative stages, to each of which is assigned a specific E-L number. The system highlights eight of these as major stages: Bud Burst (E-L 4), Shoots 10 cm (E-L 12), Flowering begins (E-L 19), Flowering (E-L 23), Setting (E-L 27), Berries pea-size (E-L 31), Véraison (E-L 35) and Harvest (E-L 38). In the context of precision viticulture, these key phenological stages and their corresponding characteristics are used as benchmarks by winegrowers and scientists to check the condition of vines, carry out necessary practices, monitor nutrients, and reduce pests and diseases. Furthermore, tracking and collecting phenotypical data of vines during the major stages is useful to estimate a vineyard's yield (Goldammer, 2015).

This research project focuses on the last key phenological stage, "Harvest" (E-L 38), which is characterized by ripened grapes having reached their potential berry size and adopted their variety's typical berry colour (Westover, 2018). Although the grapes are already ripe, the precise date of the harvest depends on their intended use and the vine-grower's desired ripeness parameters (Hellman, 2003). The aim of the paper is to model harvest-ripe grapes in 3D and to derive physical and morphological parameters, such as volume (which correlates to berry size), from these models.

2.3 Yield Prediction

Yield is another vital topic in viticulture. It is measured in tons of grapes over a vine block or other spatial unit. In specific applications, yield is also referred to as the amount of fruit on a single vine (Moyer and Komm, 2015).

Information on a vineyard's current anticipated yield enables winegrowers to check whether the yearly yield and quality goals are likely to be achieved. Yield prediction is necessary to assess when to utilize specific vineyard practices or to determine when grapes will be ready for harvest (Nuske et al., 2011). Data about physical and morphological features of grapes, such as their weight or volume, are valuable for vine experts as they help to predict yield (Hemming, 2016). Yield-prediction approaches include the in-season cluster counting method and dormant winter bud dissection (Moyer and Komm, 2015). To obtain reliable yield prediction results, yield prediction must be carried out throughout several blocks of a vineyard and throughout the seasons (Dunn, 2010). Traditionally, samples used for yield prediction are collected manually by winegrowers in the field (Nuske et al., 2014). A feature that is common to these traditional non-sensor-based approaches is their reliance on direct visual and manual in-field measurements. These traditional methods are thus very labour-intensive and allow the collection of only a limited number of samples.

The application of sensor-based technologies, such as photogrammetric approaches in combination with UAS, overcome some of these challenges as they provide a high adaptability to geographical extent and can produce highly detailed point clouds covering an entire vineyard (Rose et al., 2016). This preliminary photogrammetric study focuses on digital data and image collection associated with yield prediction. It looks at the possibility of reducing time-intensive and expensive labour, decreasing human error, and preventing destructive sampling. It takes the form of a laboratory experiment for the modelling of harvest-ripe grapes as digital 3D models based on close-range photogrammetry. The approach also allows the derivation of reliable physical and morphological parameters such as grape weight and volume.

3 Data Acquisition and Data-Modelling Methodology

The workflow of the laboratory experiment for the derivation of morphological parameters of harvest-ripe grapes is illustrated in Figure 1. The first step is to assemble the necessary equipment for data-capture. The subsequent data-capture procedure involves close-range photogrammetry to record multi-view image datasets of grapes and the manual measurement of grape features such as length, width and weight of individual grapes, which are utilized for data validation. The image datasets acquired are utilized in a multi-view 3D photogrammetric analysis to generate high-density 3D grape models. Next, the RANSAC shape-detection tool is used to derive the structure of individual grapes and parameters, such as berry diameter, from the 3D grape models. Characteristics such as the length, width, volume and weight of the digital grape clusters and of individual digital grapes are determined based on the parameters derived from the 3D model. The final step is a validation process, which involves comparing the calculated morphological parameters of the digital grapes and the manually measured parameters.

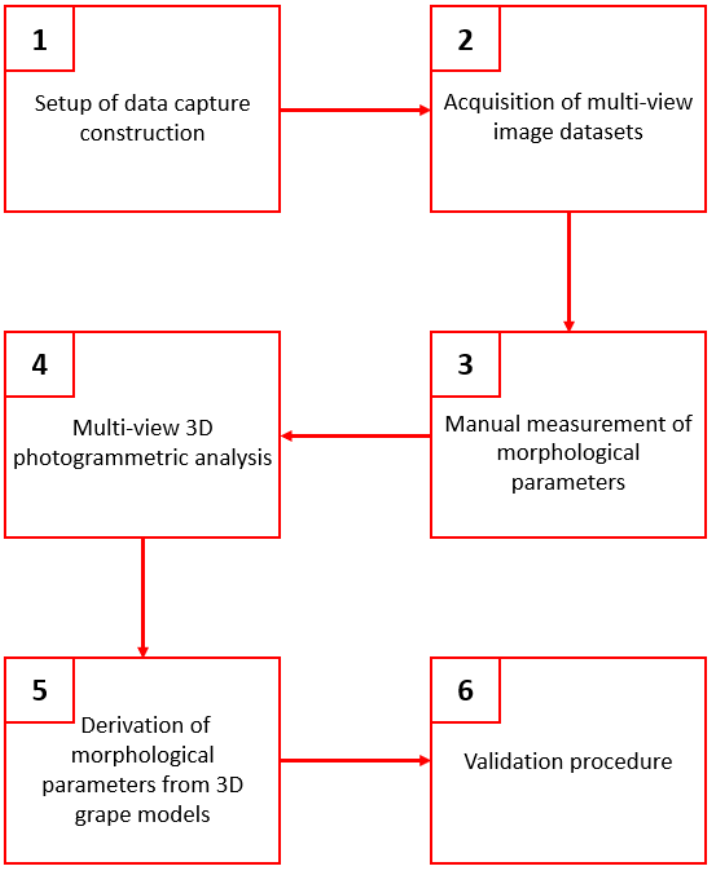

Figure 1: The laboratory experiment workflow

3.1 Laboratory Experiment Setup and Data Acquisition Process

Setting up the laboratory experiment requires gathering and installing the necessary equipment for the data capture. The equipment and objects used in the data acquisition process are:

1. Camera
    - A Sony Alpha 7r3 (Sony, 2018) was used. Relevant technical details of the camera are:
        i. 42.4megapixels
        ii. Sensor size of 35.9 times 24.0mm
        iii. Pixel dimension of 7953 times 5304pixel
2. Tripod
3. Flashers
4. Metal bars
5. Strings

6. Metal plate with holes
7. Weighing scale
8. Calliper ruler
9. Table to record measurements
10. Commercially available green and red grapes (which represent grapes from vines at the harvest stage).

The camera was used with a wide-angle lens and mounted on a tripod. The focal length of the camera was set to 90mm and the aperture to 22 for image capturing. These settings proved to provide the best results. No camera calibration was applied as the calibration is automatically estimated in the 3D modelling software.

The data-capturing construction is a framework consisting of three metal bars (see Figure 2, which illustrates the final version of the construction). The grapes are attached with strings, tape and a metal plate to the middle of the horizontal bar in such a way that they can be rotated while the tripod with the camera remains fixed. The tripod and camera are placed 1 metre away, in front of the grapes. No position marks are used in this setup, as only the relative position of the camera to the grapes is of interest, and there is a very high overlap between the images.

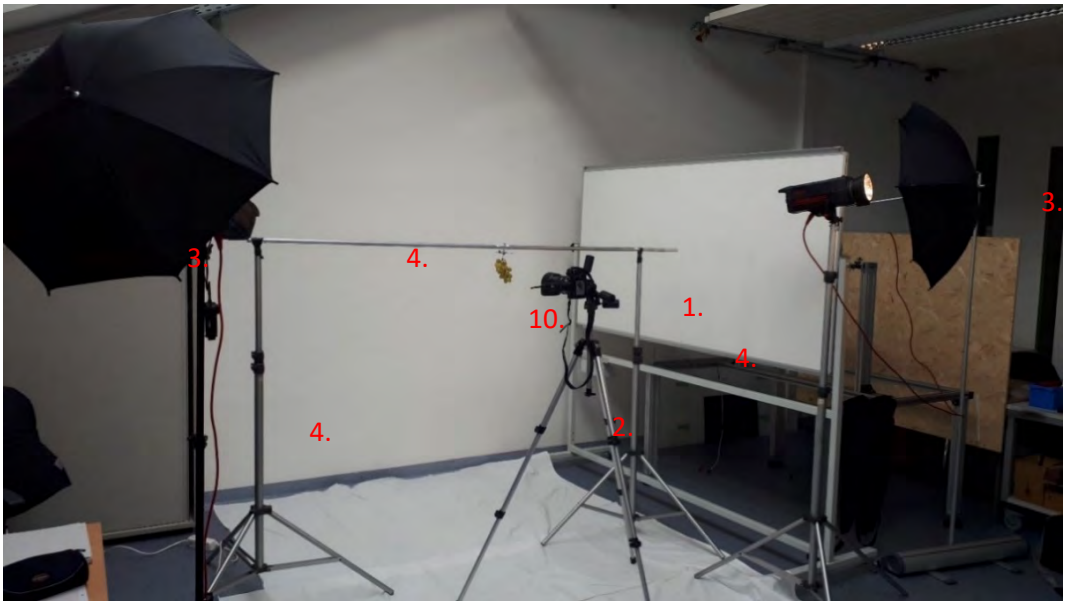

Figure 2: Data capture construction: 1. Camera, 2. Tripod, 3. Flashers, 4. Bars, 10. Grapes

The processing steps of the data-capturing procedure are shown in Figure 3. The procedure consists of two principal parts:

1. The image-capturing process applies close-range photogrammetry to generate high-resolution images of the grapes from multiple points of view. During this process, after an image is created, the grapes are rotated by a few degrees, which changes the

relative viewing angle of the camera on the grapes without moving the tripod. This ensures that images of the grapes from different points of view are recorded. The multi-view image dataset thus generated is used in the data-modelling process to create the 3D grape models.

2. The manual measurement is carried out using a calliper ruler, a weighing scale, and a table to record the measurements. First, the total weight of the grape cluster is measured and noted. Then, each grape is carefully removed from the cluster, and its length, width and weight are recorded. Figure 4 shows how the length and width of the grapes are measured. Finally, the grapes are counted and the number of grapes from the individual grape clusters are recorded in a table. Figure 5 shows the various elements required for the manual measurement of a grape cluster.

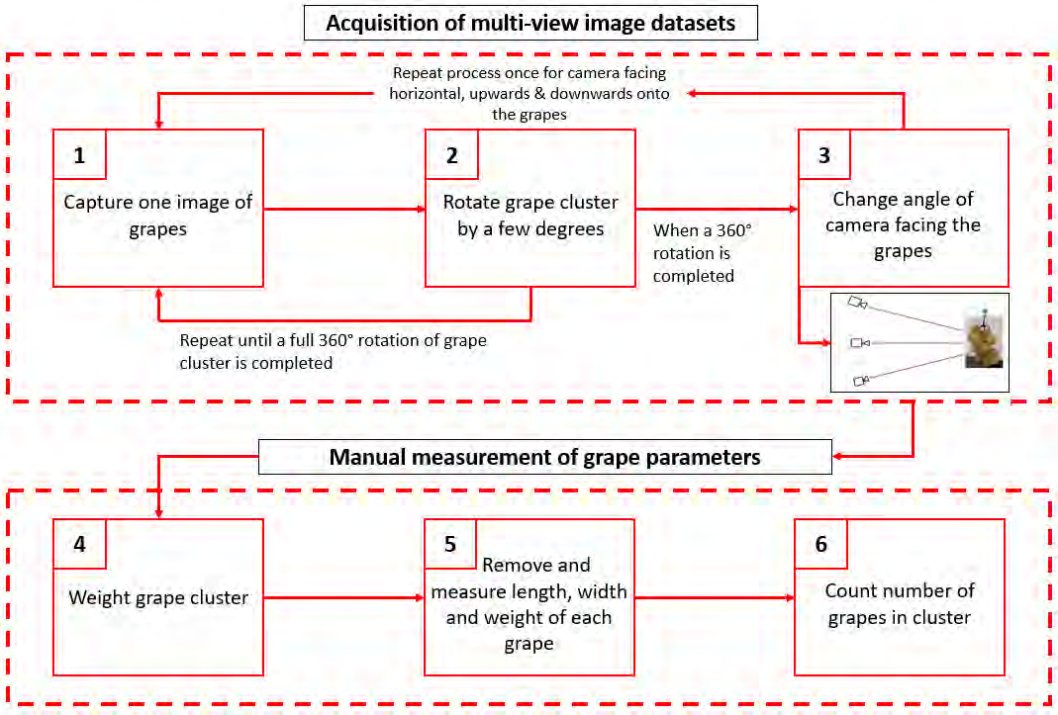

Figure 3: Workflow of the data capture process

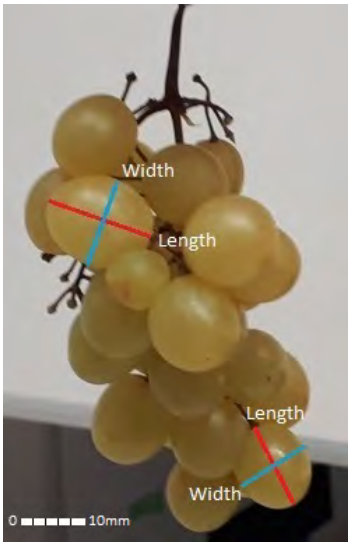

Figure 4: Measuring length and width of grapes

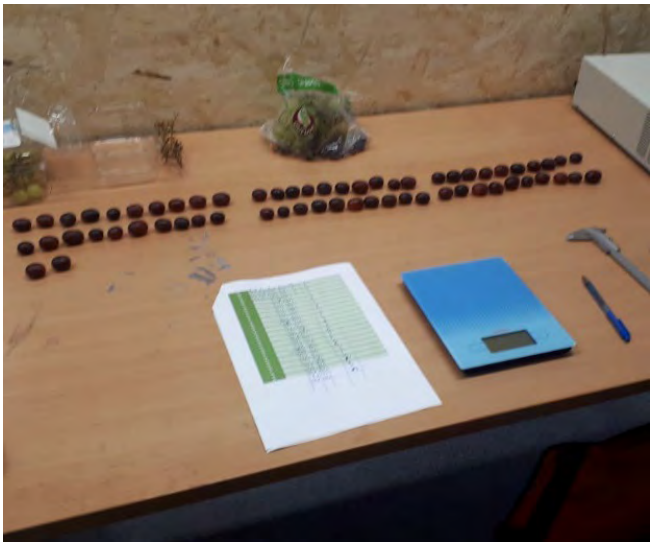

Figure 5: Material for manual measurement of grapes

3.2 Multi-View 3D Photogrammetric Analysis

The next phase of the study deals with a multi-view 3D photogrammetric analysis of the captured grape images. This multi-step procedure produces high-density photogrammetric 3D point clouds that are used to generate 3D grape models. The program Agisoft Photocan Professional© 1.4.3 (build 6529) is used (Agisoft, 2019). Figure 6 illustrates the workflow for the multi-view 3D photogrammetric analysis.

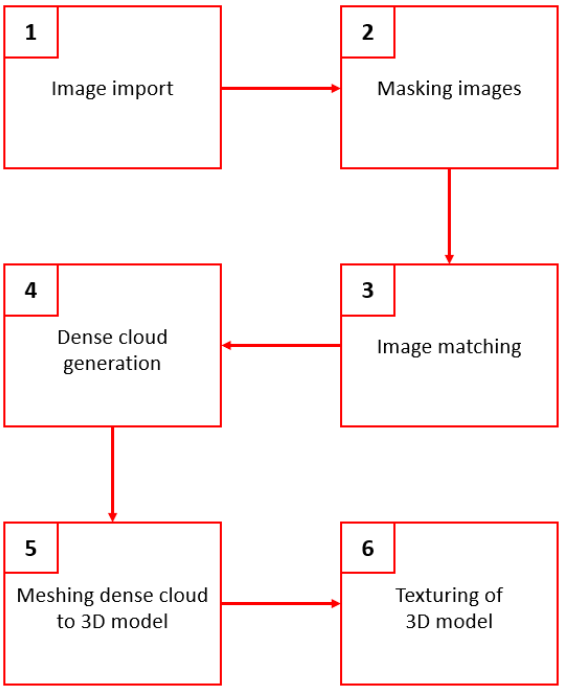

Figure 6: Workflow of the multi-view 3D photogrammetric analysis

First, the high-resolution grape images are loaded into the program. Then, using the "magic wand" tool within Agisoft Photoscan, masks are created for each image to hide such things as the bars, unnatural distortions, or white pixels representing the wall. The masking results in the 3D grape models being more precise because the modelling will only use unmasked parts of images for the calculation of the point clouds and the 3D models. The data-modelling process was tested with unmasked images, and although the resulting 3D models showed generally good results, some grapes showed 3D distortions and unnatural white strips.

Next, the images are aligned in an image-matching process. Image-matching is a prerequisite for 3D modelling of structures as it extracts 3D information from multiple overlapping images. The 3D information thus acquired can be applied to construct 3D models of the surveyed object or scene (Zhang, Xiong and Hao, 2011). The image-matching procedure uses extracted 3D information to align the images and to compute the camera positions, image orientation, and a sparse point cloud. Next, a dense point cloud is generated based on the 3D information contained in the sparse point cloud, the matched images, and the camera parameters that have been calculated. By executing a meshing algorithm, the dense clouds are meshed to 3D grape models.

Finally, a texturing process adds textures from the photographs to the corresponding parts in the previously generated 3D grape models, resulting in the final 3D models of the grapes (Figure 7, green grapes; Figure 9, red grapes). To illustrate the quality of the modelled grapes, photos of the actual grapes are also shown in Figures 8 and 10.

Figure 7: 3D model of the green grapes

Figure 8: Photo of the actual green grapes

Figure 9: 3D model of the red grapes

Figure 10: Photo of the actual red grapes

3.3 Derivation of Morphological Parameters from 3D Grape Models

The next step of the methodology is to identify the shapes of the individual grapes in the 3D models and to derive the physical and morphological parameters of single grapes and of grape clusters. Data such as their weight and volume are important for winegrowers and wineries as they can be utilized to predict yield (Hemming, 2016).

In order to identify the shapes of individual grapes, the RANSAC shape detection plugin (Schnabel, Wahl and Klein, 2007) of the program CloudCompare (CC) version v2.10-alpha [64-bit] (CloudCompare, 2019) is deployed to fit spherical shapes into detected grapes in the 3D models. If a sphere-like shape is found in a 3D model, the corresponding part of the model is separated, colour-coded, and a sphere is placed at that location. The grapes detected in the 3D models are shown in Figures 11 (green grape model) and 12 (red grape model). The grapes in these figures are shown in different hues to allow easier visual distinction between single grapes.

The CC plugin also calculates parameters of these shapes, such as the radius. The radius (r) of an identified digital grape is, by definition, half the grape's width. Thus the width (b) of a 3D grape is derived from its radius. Next, the length (a) of each modelled grape is determined using its width and the length–width ratio (c) of the actual grape. The volume of the digital grapes is calculated using the volume formula for oblate ellipsoids (Eq. 1):

Eq. 1: Ellipsoid volume formula

$$V = \frac{4}{3} * \pi * \left(\frac{b}{2}\right)^2 * \left(\frac{a}{2}\right) = \frac{4}{3} * \pi * r^2 * (r * c)$$

Variable "V" is the volume, and the variables "a" and "b" represent the length and width, respectively. We assume that $\frac{b}{2} = r$ and $\frac{a}{2} = r * c$ where r is the radius calculated by the tool, b is the grape width (i.e. the small semi-axis of the ellipsoid), a is the large semi-axis or the grape length, and c is the mean ratio of length and width measured manually on actual grapes.

In the next step, the mean length and width, length variance and width variance, mean volume and volume variance of the grapes, and total volume of the 3D grape clusters are determined. To validate these derived morphological parameters of the digital grapes, the same parameters are calculated for the actual grapes using the manual measurements. Since the weight of the actual grapes was also measured in the data acquisition process, the density of these grapes can be calculated using the formula (Eq. 2):

Eq. 2: Density formula

$$\varrho = \frac{W}{V}$$

where "ϱ" (Rho) is the density, "W" is the weight, and "V" is the volume. The mean density of the green and red grapes is determined. Now, the weight, mean weight and weight variance of the modelled grapes are calculated using the mean density values of the actual grapes. The results of these calculations are given in Table 1. The values in brackets in Table 1 are the total volume and weight of the digital red grapes, as if all 62 grapes had been detected. For the

missing grapes, the mean volume and weight values of the other 3D modelled red grapes were used as proxies.

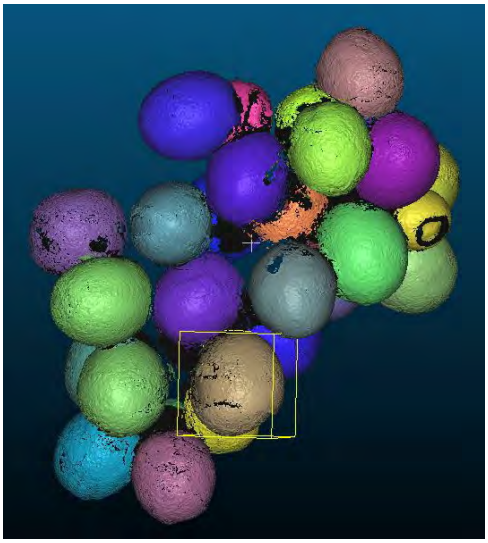

Figure 11: Shapes of the detected green grapes

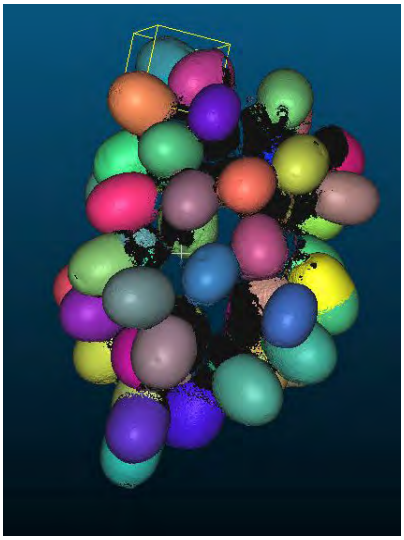

Figure 12: Shapes of the detected red grapes

Table 1: Calculated morphological parameters of actual and digitally derived green and red grapes. * Values in brackets are the total values, as if all actual grapes had been detected

Parameter [unit]	Green grapes		Red grapes	
	Actual grapes	Digital grapes	Actual grapes	Digital grapes
Number of grapes [-]	29	29	62	55
Mean Length [mm]	21.18	21.18	24.11	24.11
Length Variance [mm]	1.46	1.07	3.81	1.22
Mean Width [mm]	18.75	18.75	18.41	18.41
Width Variance [mm]	1.04	0.94	2.06	0.93
Total Volume [mm³]	115,444.02	115,005.25	269,494.7	239,288.22 (269,743.08)*
Mean Volume [mm³]	3,980.83	3,981.05	4,346.69	4,350.69
Volume Variance [mm³]	639.16	556.33	1,565.36	684.93
Total Weight [g]	138.00	137.48	346.00	307.22 (346.32)*
Mean Weight [g]	4.76	4.74	5.58	5.59
Weight Variance [g]	0.76	0.67	2.01	0.88
Mean Density [g/mm³]	0.001195	-	0.001284	-

4 Results and Discussion

The laboratory experiment was performed three times. The setup and methodology described in this paper were followed in experiments 2 and 3 (the setup for experiment 1 was smaller), and the quantification was carried out only in the third experiment. In total, 6 grape clusters, one green and one red grape cluster per experiment, were examined. The final 3D grape models are illustrated in Figure 7 and Figure 9, and the quantification results are shown in Table 1.

The results of the approach demonstrate the reconstruction of 3D grape models under laboratory conditions. The visual comparison of the models shown in Figure 7 and Figure 9 with the actual grapes in Figure 8 and Figure 10 shows that the modelled digital grapes are very similar to their actual counterparts. However, the comparison also reveals that some digital grapes were not correctly reconstructed, which can be seen in certain deformations in the digital grapes. It can be concluded that the process used in this laboratory experiment worked well for detecting grapes: the results of the shape-detection illustrated in Figure 11, Figure 12, and row 2 "Number of grapes [-]" in Table 1 show that all 29 green grapes were detected. In addition, 55 of the 62 red grapes were correctly identified, an accuracy of 88%. However, the shape-detection procedure shows difficulties in identifying strongly elliptical grapes, such as the 7 undetected red grapes. Furthermore, the methodology is reliable for the derivation of physical and morphological parameters from 3D grape models. The calculated total weight, displayed in row "Total Weight [g]" in Table 1, of the digital green grape cluster (137.48g) differs by just 0.52g (0.4%) from the weight of the actual green grape cluster (138.0g). The estimated total weight of the digital red grape cluster (346.32g) differs by just 0.32g from its actual counterpart (346.0g).

The results of this work can be compared with the measurements of Coetzee and Lombard (2013), who examined 300 berries from 37 grape clusters to determine specific grape parameters. They calculated an average grape cluster weight of 101.3g, which differs significantly from the estimated total grape cluster weights presented in this paper (138.0g for the digital green grape cluster; 346.0g for the digital red grape cluster). The average grape densities (1,130kg/m³ in Coetzee and Lombard (2013); 1,195kg/m³ (green grapes) and 1284kg/m³ (red grapes) in this study) are also significantly different. These disparities can be attributed to the use of differently sized grapes in the two studies. Coetzee and Lombard (2013) calculated an average grape length of 14.6mm and grape width of 12.5mm, whereas the mean grape lengths in this work were 21.18mm (green grapes) and 24.11mm (red grapes), and the mean grape widths were 18.75mm (green grapes) and 18.41mm (red grapes).

Some of our results were inconclusive. The calculated variance values differ greatly between the various parameters measured for the digital and the actual grapes. An example is the large difference in length variance, which is 0.39mm for the digital green grapes and the actual grapes, and 2.59mm for the red grapes. The large variance between the digital and the actual grapes is thought to be caused by the shape detection method we applied, which utilized spheres to approximate the grape shapes. We also experimented with using cylinders to detect grapes, but this proved inadequate as it resulted in a model of just 10 grapes.

Several problems and limitations were identified. The approach showed difficulties with the accurate reconstruction of misshapen or strongly elliptical grapes. Examples are highlighted by red circles in Figure 13 and Figure 14. These grapes could be correctly detected with the use of LiDAR-based systems. Another technology which can be applied to analyse the shape of any grape is described in American Society for Horticultural Science (2009). An advantage of the SigmaScan®-based approach described there over the method presented in this paper is the grapes' independency from geometry and spatial position through the measurement of grapes based on difference in colour between the surveyed grape and the background. Additional errors such as holes in parts of stems were found because adequate point density cannot always be achieved for the modelling of thin structures. Another limitation is the immobility of the data-capture setup. It took several attempts to find an appropriate procedure and settings. Furthermore, a new construction would need to be built if an entire row of vines was to be simulated and modelled.

The results of our preliminary laboratory experiment indicate that close-range photogrammetry can be applied to generate 3D grape models and that parameters such as the volume of the grape can be derived from these digital models.

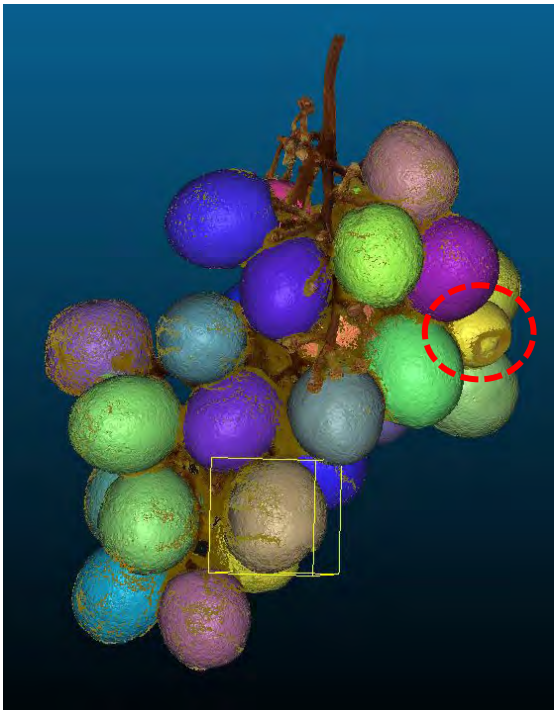

Figure 13: Difficulties detecting misshapen grapes

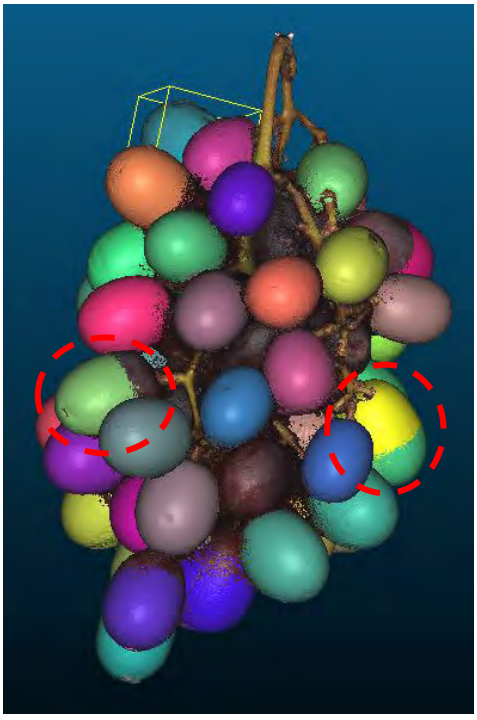

Figure 14: Incorrectly identified elliptical grapes

5 Conclusions and Future Work

In this paper we conceptualized and modelled 3D grapes and used these models to derive physical and morphological parameters. In the laboratory experiment, a special data-capture setup was constructed to record multi-view high-resolution image datasets of commercially available green and red grapes, representing grapes at harvest stage (E-L 38). The data-modelling process focused on the generation of high-resolution 3D grape models, the derivation of parameters from them, and the comparison of the parameters for 3D grape models and actual grapes. The approach shows that close-range photogrammetry can be applied in a lab to create high-resolution 3D grape models and to derive reliable physical and morphological parameters.

In a future project, a similar approach could be applied in-field by, for example, creating a system of multiple cameras mounted on an unmanned autonomously moving vehicle, such as a UAS, which generates close-range multi-view image datasets. These datasets could then be utilized to generate 3D models of grapes on the vines, which in turn could be used to derive parameters such as grape volume to estimate the yield of the grapes.

Acknowledgments

The authors would like to thank the three anonymous reviewers and editor Mary Rigby for their valuable input into the content of this paper, which certainly improved the quality of it.

References

Agisoft. (2019). Professional Edition. Retrieved from https://www.agisoft.com/features/professional-edition/

American Society for Horticultural Science. (2009). Grape shapes. Retrieved from https://www.eurekalert.org/pub_releases/2009-02/asfh-gs021709.php

Centinari, M. (2018). Grapevine Bud Break 101 [Blog post]. Retrieved from https://psuwineandgrapes.wordpress.com/2018/05/14/grapevine-bud-break-101/

CloudCompare (version 2.10-alpha) [GPL software]. (2019). CloudCompare - Open Source project. Retrieved from http://www.cloudcompare.org/

Coetzee, C. and Lombard, S. (2013). The destemming of grapes: Experiments and discrete element modelling. *Biosystems Engineering.* 114(3), 232-248.

Dunn, G. M. (2010). *Yield Forecasting* [Fact sheet]. Retrieved from https://www.wineaustralia.com/getmedia/5304c16d-23b3-4a6f-ad53-b3d4419cc979/201006_Yield-Forecasting.pdf

Goldammer, T. (2015). *The grape grower's handbook*. 2nd edition. USA: Apex Publishers.

Hellman, E. W. (2003). Grapevine Structure and Function. Retrieved from https://www.growables.org/information/LowChillFruit/documents/GrapeExtOrg.pdf

Hemming, R. (2016). Wine by numbers: viticulture, part one. Retrieved from https://www.jancisrobinson.com/articles/wine-by-numbers-part-one

Maniak, S. (2004). *Datenaustausch in geographischen Informationssystemen.* [Data exchange in geographic information systems]. Düren, Germany: Shaker, 5-14.

Moyer, M. M. & Komm, B. (2015). *Vineyard Yield Estimation.* Washington State University Extension. Retrieved from https://www.vineyardteam.org/files/resources/Vineyard%20Yield%20Estimation-%20WSU.pdf

Nuske, S., Achar, S., Bates, T., Narasimhan, S. G. & Singh, S. (2011). Yield estimation in vineyards by visual grape detection. *IEEE International Conference on Intelligent Robots and Systems.* 2352-2358. doi:10.1109/IROS.2011.6095069.

Nuske, S., Wilshusen, K., Achar, S., Yoder, L., Narasimhan, S. & Singh, S. (2014). Automated Visual Yield Estimation in Vineyards. *Journal of Field Robotics, 31*(5), 837-860.

Poupin, M. J., Matus, J. T., Leiva-Ampuero, A. & Arce-Johnson, P. (2011). *The Flowering Process and its Control in Plants: Gene Expression and Hormone Interaction.* 1st edition. Kerala, India: Research Signpost, 173-197.

Rose, J., Kicherer, A., Wieland, M., Klingbeil, L., Töpfer, R. & Kuhlmann, H. (2016). Towards Automated Large-Scale 3D Phenotyping of Vineyards under Field Conditions. *Sensors, 16*(12), 1-7.

Schnabel, R., Wahl, R. and Klein, R. (2007). Efficient RANSAC for Point-Cloud Shape Detection. *Computer Graphics Forum*, *26*(2), 214-226.

Sony (2018). Sony α7R III 35 mm full-frame camera with autofocus. Retrieved from https://www.sony.co.in/electronics/interchangeable-lens-cameras/ilce-7rm3/specifications

Westover, F. (2018). Grapevine Phenology Revisited. Retrieved from https://www.winesandvines.com/features/article/196082/Grapevine-Phenology-Revisited

Wine Institute (2019). World Wine Production by Country. Retrieved from https://personalpages.manchester.ac.uk/staff/fumie.costen/pastwork/grapes/XiaoWenyu.pdf

Zhang, Y., Xiong, J., & Hao, L. (2011). Photogrammetric processing of low-altitude images acquired by unpiloted aerial vehicles. *Photogrammetric Record. 26*(134), 190-211.